*Anal. Bioanal. Electrochem., Vol. 15, No. 5, 2023, 382-393*
*https://www.doi.org/10.22034/abec.2023.705136*

*Analytical &*
*Bioanalytical*
*Electrochemistry*

2023 by CEE
www.abechem.com

*Full Paper*

# Anticorrosive Properties of Nickel-Alumina Composite Coatings on A Steel Substrate

**Rekaik Mouna,[1] Azzouz Noureddine,[2] and Ferkhi Mosbah[3]**

*[1]Process Engineering Department, Yahia Farés Médéa University, Materials-Environment Interactions Laboratory (LIME) Jijel, Algeria*
*[2]Department of Process Engineering, M.S.B.Yahia Jijel University, Laboratory of Materials-Environment Interactions (LIME) Jijel, Algeria*
*[3]Department of Chemistry, University M.S.B.Yahia Jijel, Laboratory of Material-Environment Interactions (LIME) Jijel, Algeria*

*Corresponding Author, Tel.: +213559561263
E-Mail: mrekaik@yahoo.fr

*Received: 4 December 2022 / Received in revised form: 8 May 2023 /*
*Accepted: 20 May 2023 / Published online: 31 May 2023*

---

**Abstract-** Herein, an electroplating method has been developed in order to improve the anti-corrosion properties of steel. Ni-based compounds to which solid $Al_2O_3$ particles have been electrochemically inserted. Nickel-alumina mixtures were deposited on steel substrates from the electroplating bath using different concentrations of $Al_2O_3$. The electrochemical corrosion tests of the samples were carried out in two different solutions 0.5 M $K_2SO_4$ and 0.5 M NaCl. Structural and morphological analyzes were carried out by X-ray diffraction (XRD) and scanning electron microscopy (SEM) coupled to microanalysis (EDAX) analyses respectively. The electrochemical behavior of co-electrodeposited coatings (Ni-$Al_2O_3$) in corrosive solutions was followed using potentiodynamic methods and electrochemical impedance spectroscopy (EIS). The various tests carried out under working conditions revealed that the $Al_2O_3$ particles added to the bath have a beneficial effect on the electrochemical behavior of the steel by reducing its tendency to corrosion. In this work, we were also able to determine the optimal concentration leading to significant inhibition of the steel tested. This synthesized and studied concentration related to $Al_2O_3$ was evaluated at around 20 $g.L^{-1}$.

**Keywords-** Electrodeposition; Composite coating Ni-$Al_2O_3$; Electrochemical Impedance Spectroscopy (EIS); Potentiodynamic polarization; Co-deposition

---

## 1. INTRODUCTION

Coatings with composite materials against corrosion have been the subject of much research in recent years. These composite materials can be produced by the deposition of inert particles in a metal matrix from an electrolytic bath considered as the metal matrix of the composite coating [1]. The presence of these particles changes the structure and composition of the coating, giving it a map, new properties, and new features [2]. The metal matrix may well see its hardness, corrosion resistance, and many other properties increased by the appropriate choice of embedded particles.

It should be noted that it is the choice of particle size and composition which has a direct impact on the implementation of the process and lead to a quality of a finished coating [3].

The reasons for using nickel in the corrosion protection of steel are, first, the ability of this to provide cathodic protection to steel and low nickel corrosion rate in non-aggressive environments, but also reasonable price and simple application on the steel surface by electrodeposition. Nickel has fairly high corrosion resistance, for which reason it is used in the protection of steel, the average length of life of such coatings is limited because of the aggressive nature of some media, especially, those containing industrial pollutants. This is why we sought an improvement in corrosion resistance by the incorporation of inert particles in the metal matrix during electrodeposition. Allowing, thus, obtaining composite materials with superior properties, such as resistance to corrosion and extended wear, catalytic, magnetic, and hardness [2, 4-13]. In addition, the method of co-electroplating with oxide particles is inexpensive for many uses .

In this regard, the most commonly used particles are oxides such as Alumina [13], Silica [14], carbides such as Tungsten carbide [8], Zirconium carbide [15], and Silicon carbide [16-18], metals and polymers [19-27]. As for the parameters influencing the properties of the solid particles on such an electrode, the main electrodeposition parameters are; the electrolyte composition, current density, temperature, pH, and the concentration of particles in the bath [28-30].

These co-deposition techniques have been developed for a large number of materials including, alloy, semiconductor, superconductor oxides, and conductive polymers .

With the aim of the synthesis of new composite materials such as Ni-$Al_2O_3$, in this work, we will use the co-electrodeposition method to ameliorate the quality of the surface of steel against its corrosion in aggressive solutions.

## 2. MATERIALS AND METHODS

### 2.1. Experimental method

The sample material used in our work is ordinary steel (black plate). The samples were recovered in the form of plates of dimensions (25×40×1.5) mm of the same product in order to ensure the reproducibility and validity of the results of our tests. The development of the nickel deposits and the deposits of nickel-alumina was carried out at the level of the University of Jijel.

The composition, the concentrations, and the conditions used for the various electrolytic deposits are shown in Tables 1 and 2 respectively.

**Table 1.** Composition of the bath for the deposition of $Ni-Al_2O_3$

| | **constituents** | | | | |
|---|---|---|---|---|---|
| | **$NiCl_2.6H_2O$** | **$NH_4Cl$** | **NaCl** | **$H_3BO_3$** | **$Al_2O_3$** |
| **Content [$g.L^{-1}$]** | 11.885 | 12.303 | 4.091 | 6.183 | 0, 20 and 30 |

**Table 2.** Conditions of bath co-deposition

| **Operating Conditions** | | |
|---|---|---|
| **Temperature** | **Voltage** | **time deposit** |
| 40± 2°C | 4 V | 75 min |

A three-electrode setup and 100 ml solutions are used. The anode is nickel, while the cathode is steel separated by approximately 2 cm. The cathode (working electrode) is connected to the negative pole of a current (or voltage) generator and the anode is connected to the positive pole via a multimeter. The cell is placed on a heated magnetic stirrer with a stirring device. The reference electrode is a saturated calomel electrode (SCE).

Before electrochemical measurements, the surfaces of composite nickel-alumina deposits were examined with X-ray diffraction (XRD) and scanning electron microscope (SEM). The electrochemical measurements have been carried out by a potentiostat-galvanostat VoltaLab 40 type Radio-Meter PGZ 301 with an integrated transfer function, controlled by the software VoltaMaster 4. A cell comprises a three-electrode assembly, the steel coated with the composite deposit $Ni-Al_2O_3$ as the working electrode (WE), a cylindrical grid of large surface surrounding the working electrode as against electrode (AE), and a saturated calomel electrode (SCE) as a reference electrode.

The corrosion tests were carried out at ambient temperature on solutions of potassium sulfate ($K_2SO_4$ 0.5 M) and solutions of sodium chloride (NaCl 0.5 M) under air and without stirring. Then, the potensiodynques measurements were carried out in a potential range between -800 mV to +600 mV/ECS, with a scanning speed equal to 0.25 $mV.s^{-1}$. The working electrode (WE) potential reached stability after waiting 30 minutes. The individual specimens corrosion current density ($i_{corr}$) was determined by extrapolating the anode and cathode Tafel curves.

## 3. RESULTS AND DISCUSSION

### 3.1. Scanning Electron Microscopy (SEM)

Scanning Electron Microscopy allows having an idea about the morphology of the surface of our samples. Figure 1 shows the composite deposit microstructure Ni-$Al_2O_3$ alumina having concentrations of 0, 20, and 30 g. $L^{-1}$.

For 0 g. $L^{-1}$ of $Al_2O_3$, the grain of nickel are spherical, large grains, and uniform size (Figure 1a). However, with the addition of $Al_2O_3$ particles at different concentrations, the shape of the nickel grains became nodular (Figure 1b and c) and their size became smaller and smaller with increasing nickel content Alumina. However, increasing the concentration of alumina particles in electrolytic baths, below a certain limit, leads to agglomeration due to the high surface energy of the particles and the more intense interaction between them [31]. These agglomerates are incorporated and distributed unevenly over the entire surface of the electrode.

Some researchers studied the co-deposition of the inert particles by electroplating and found that there is a strong tendency among agglomeration of particles due to their high activity. If the particles are not well dispersed in the bath, they are likely to be incorporated as aggregates in the metal matrix [32].

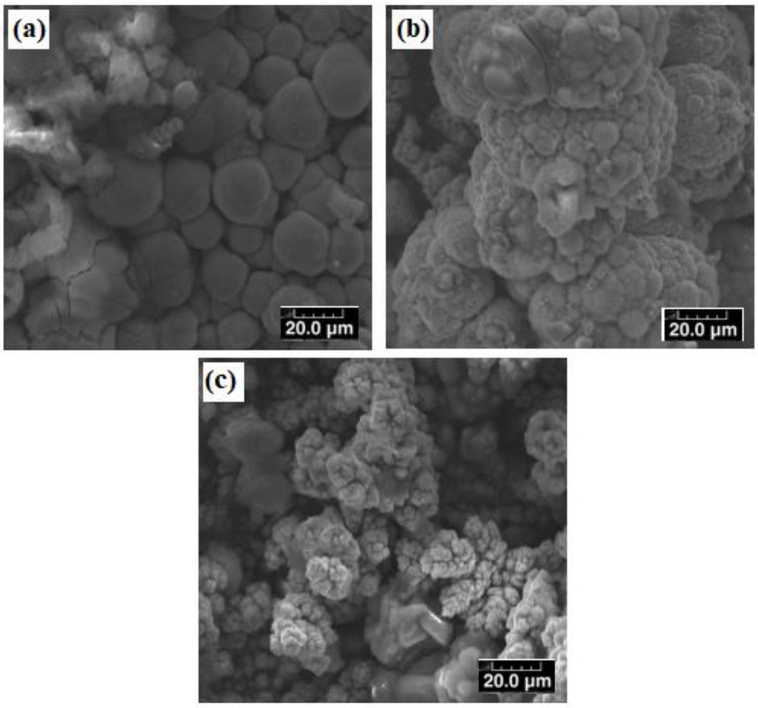

**Figure 1.** SEM micrographs of the surface of the deposit of pure Ni (a) and composite coatings of Ni-$Al_2O_3$, obtained with different concentrations of $Al_2O_3$ particles in the plating bath 20 g $L^{-1}$ (b) and 30 g $L^{-1}$ (c)

### 3.2. X-ray diffraction (XRD)

The plates coated in baths with concentrations of 0, 20, and 30 g. $L^{-1}$ of $Al_2O_3$ was analyzed by X-ray diffraction with a length of $\lambda = 1.5406$ Å. Figure 2 represents the diagrams of the diffraction of samples obtained by the deposit of the composite Ni-$Al_2O_3$.

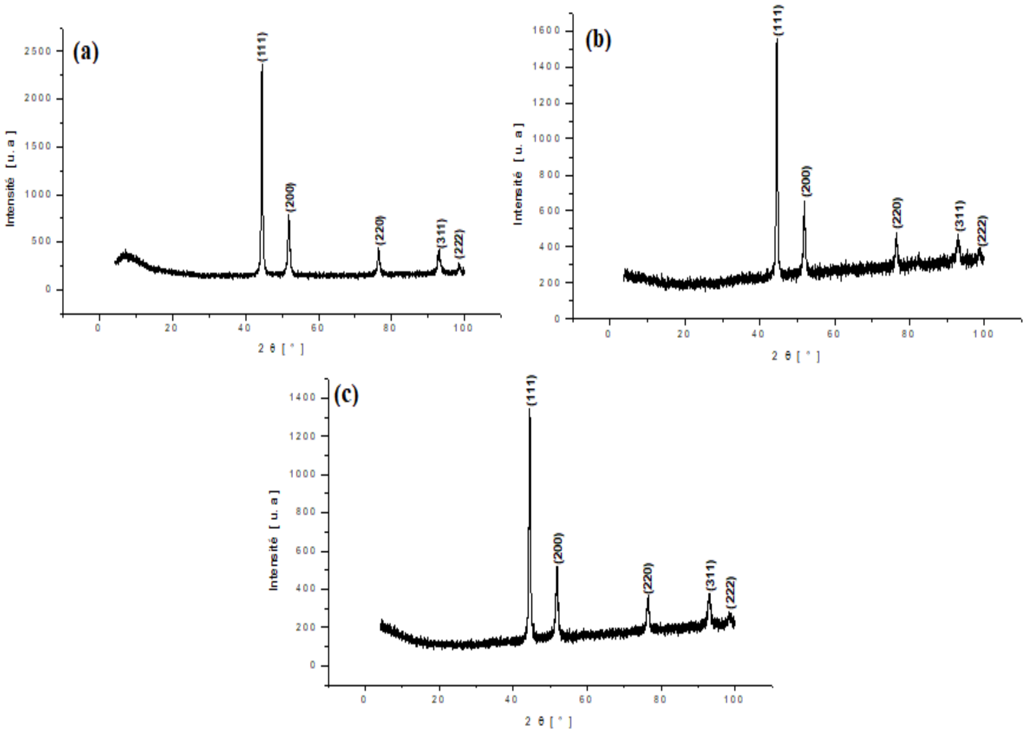

**Figure 2.** X-ray diffractions of a sample coated in the bath in the presence of 0 g. $L^{-1}$ (a); 20 g. $L^{-1}$ (b) and 30 g $L^{-1}$ (c) $Al_2O_3$

Whatever the alumina concentration added to the electroplating bath, the XRD diagrams obtained at different concentrations of $Al_2O_3$ clearly show the shape of the Ni phase which crystallizes in the space group Fm3m cubic system. These diffractograms thus confirm the presence of a single-phase structure. Gheorghies and et al [33] also showed similar results in Ni-alumina nano-composites. It is noted that the relative intensity of the (111) plane is high whereas the alumina is absent, however, the intensity of the (200) plane increased after alumina additions. This can be allocated to the preferential growth of Ni grains in the presence of alumina [2]. Also, according to Wen-Ya Li and et al [34] the low intensities of the $Al_2O_3$ peak are because the $Al_2O_3$ particulates are almost covered by the Ni particulates.

The shift of a peak with respect to its theoretical position is attributed to internal stresses in the films, that is to say, the closer the Ni peaks are to their theoretical position, the more this suggests that these films have fewer stresses.

### 3.3. Potentiodynamic polarization

The potentiodynamics polarizations coated steel of different concentrations of alumina in the above-mentioned settings after 30 minutes of immersion are reported in Figure 3.

The values of corrosion potentials ($E_{corr}$) and corrosion current densities ($i_{corr}$) are obtained from the processing of the polarization curves (extrapolation method straight Tafel –Table 3-). The corrosion rate values ($V_{corr}$) are calculated from the following formula:

$$V_{corr} = 3.27\frac{i_{corr}.M}{\rho.n} \qquad (1)$$

With:

$V_{corr}$: Corrosion rate [mm. $an^{-1}$];
$i_{corr}$: Current density [mA. $cm^{-2}$];
M: Molecular weight [g. $mol^{-1}$];
ρ: Density [g. $cm^{-3}$];
n: Valence [1].

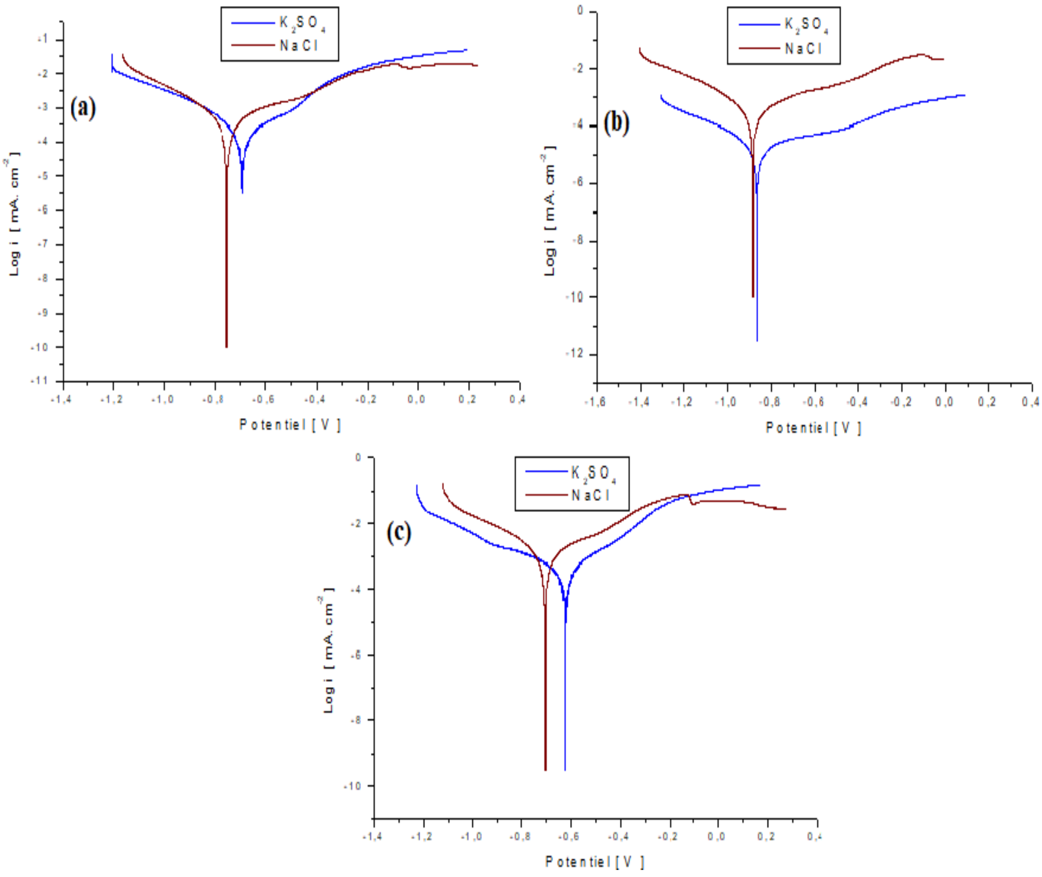

**Figure 3.** Polarization curves for a steel plate coated in a bath without alumina (a), with 20 g. $L^{-1}$ (b) and 30 g. $L^{-1}$ (c) of $Al_2O_3$ in 0.5M $K_2SO_4$ and 0.5 NaCl

**Table 3.** Values of electrochemical parameters in a bath of 0; 20 and 30 g. $l^{-1}$ $Al_2O_3$ in $K_2SO_4$ and NaCl solutions

| **Concentration of $Al_2O_3$ [g/l]** | **Solutions** | **Values** | | |
|---|---|---|---|---|
| | | ***$E_{corr}$ [mV]*** | ***$i_{corr}$ [$mA.cm^{-2}$]*** | ***[$mm.an^{-1}$]*** |
| **0** | **$K_2SO_4$** | -687.87 | 0.244 | 2.86 |
| | **NaCl** | -752.19 | 0.632 | 7.398 |
| **20** | **$K_2SO_4$** | -864.86 | 0.024 | 0.277 |
| | **NaCl** | -886.18 | 0.632 | 3.676 |
| **30** | **$K_2SO_4$** | -623.92 | 0.469 | 5.491 |
| | **NaCl** | -704.09 | 1.062 | 12.433 |

Following the observations after immersion in solutions of 0.5 M NaCl and 0.5M $K_2SO_4$, and viewing the nature of nickel coatings on steel (cathode coatings), the form of corrosion encountered in cases where the electrolyte is NaCl is localized corrosion. It consists of local attacks of the passive film due to the presence of pores on the deposits; against by, in the case where the electrolyte is $K_2SO_4$, the form of corrosion is uniform (the attack is spread over the entire surface).

The polarization curves plotted for the electrodes covered with the composite deposit Ni-$Al_2O_3$ show that there is a change in the corrosion potential of the material treated. The composite deposition Ni-$Al_2O_3$ moves the corrosion potential to values less noble (cathodic displacement) when compared to that of the steel in the two solutions (NaCl and $K_2SO_4$). However, the offset of this potential is remarkably more negative for the submerged slides in NaCl than for those immersed in $K_2SO_4$ [1].

From the polarization curves obtained on the coated slides immersed in $K_2SO_4$, we see a decrease in the corrosion current density as a function of the added alumina concentration in the nickel bath until 20 $g.L^{-1}$. After this value; we see a further increase in the current density. According to (Table 3) we see a progressive decrease in velocity over corrosion of the added alumina concentration in the bath until an optimal value corresponds to the concentration of 20 $g.L^{-1}$. Beyond this optimum, there is a new gradually increasing corrosion rate. This is explained by the presence of alumina particles in the nickel matrix, which fills the pores existing therein and, in the interval [0,20] $g.L^{-1}$. Beyond 20 $g.L^{-1}$, there is an increase in corrosion rates that can be interpreted by the excessive presence of particles of $Al_2O_3$ in the electrodeposited nickel structure, which disrupts the efficiency of the film thus constituted by a recovery rate of $Al_2O_3$ more porous than the case of Ni less than alumina.

In another aggressive solution, the same studies were carried out in the NaCl solution, we observe the same results as before. A gradual decrease in the corrosion rate with the concentration of alumina added in the bath until an optimum value of 20 g. L$^{-1}$ is reached. Beyond this concentration value, a further increase in the corrosion rate is distinguished at 30 g. L$^{-1}$, which can be explained by the presence of defects and dislocations and/or chemical heterogeneities in the metal matrix and/or by non-uniform incorporation of the particles due to the formation of agglomerates.

### 3.4. Electrochemical Impedance Spectroscopy (EIS)

The impedance measurements are carried out after 30 minutes, 2, 4, 6, and 24 hours of immersion in two different media $K_2SO_4$ (0.5M) and NaCl (0.5M) at room temperature, with air and without agitation. The impedance measurements are carried out in a frequency range between 100 kHz and 10 mHz and under an amplitude of 10 mV with respect to the corrosion potential, the number of points per decade: 10 points/decade, and an integration time: 4 sec. Nyquist diagrams are recorded at different immersion times and at different concentrations of alumina, added in $K_2SO_4$ and NaCl solutions, and are shown in Figure 4.

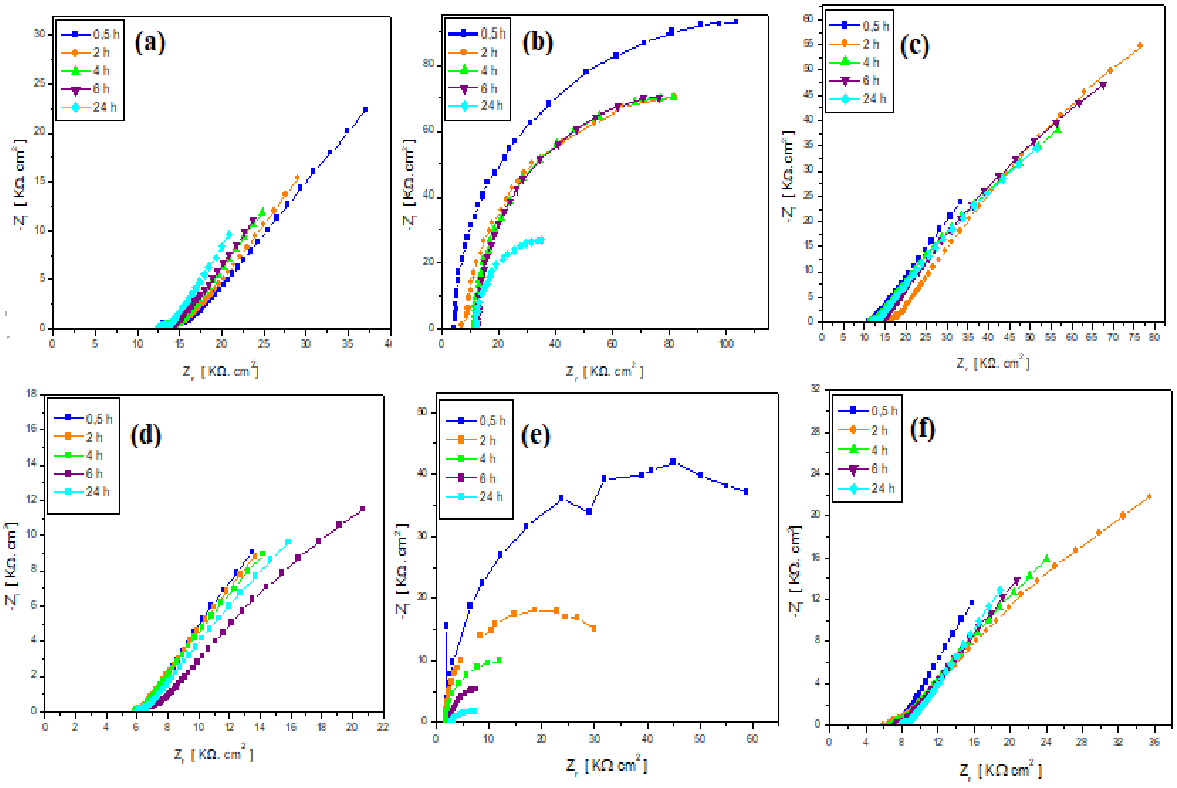

**Figure 4.** Nyquist plot of the impedance spectrum of a steel plate coated in a bath of 0 g. L$^{-1}$ (a); 20 g. L$^{-1}$ (b) and 30 g. L$^{-1}$ (c) of $Al_2O_3$ in 0.5M $K_2SO_4$ and of 0 g. L$^{-1}$ (d); 20 g. L$^{-1}$ (e) and 30 g. L$^{-1}$ (f) of $Al_2O_3$ in 0.5 M NaCl after various immersion times

For samples covered by the composite Ni-$Al_2O_3$ deposition with different alumina concentrations: 0 and 30 ($g.L^{-1}$), the electrochemical impedance spectra obtained after various immersion times in both electrolytic media exhibit two semicircles; the first semi-circle at high frequencies characterized the coating layer and the second at low frequency indicates the diffusion phenomena called Warburg impedance.

For the sample coated with the composite deposition, with the concentration of $Al_2O_3$ of 20 $g.L^{-1}$, we see the presence of a single capacitive loop, reflecting the layer deposited with a resistance value ($R_{rev}$) very large compared to other samples. This reflects the effect of the protective film of this coating concentration of $Al_2O_3$.

The simulation of the experimental impedance diagrams was obtained; equivalent circuits of the RC type are adopted (Figure 5). The simulation was performed using ZSimpWin Version 3.21 software.

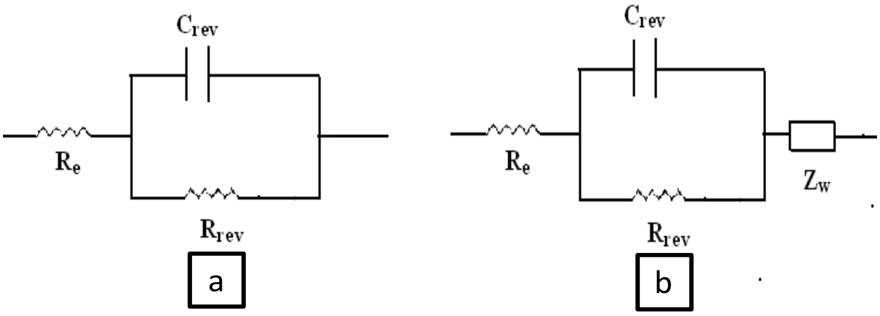

**Figure 5.** The equivalent circuit diagram in system Ni-$Al_2O_3$ / electrolyte at different concentrations of $Al_2O_3$ particles in the deposition bath 20 g. $L^{-1}$ (a) 0 and 30 g. $L^{-1}$ (b)

The parameters obtained after the simulation are shown in Tables 4 and 5

**Table 4.** Value characteristic of metal-coated resistors recorded as a function of immersion time in $K_2SO_4$ and NaCl

| **Solutions** | **Concentration of $Al_2O_3$ [g/l]** | **Time (h)** | | | | |
|---|---|---|---|---|---|---|
| | | ***0.5*** | ***2*** | ***4*** | ***6*** | ***24*** |
| **$K_2SO_4$** | **0** | 1.70 | 1.357 | 1.075 | 0.984 | 0.567 |
| | **20** | 198.1 | 158.2 | 155 | 149.8 | 60.1 |
| | **30** | 15.36 | 0.926 | 0.631 | 0.623 | 0.504 |
| **NaCl** | **0** | 8.796 | 5.458 | 4.039 | 0.613 | 0.304 |
| | **20** | 81.28 | 36.31 | 18.84 | 13.70 | 12.16 |
| | **30** | 19.41 | 1.065 | 0.653 | 0.522 | 0.427 |

**Table 5.** Value of the capacitance of the coating obtained metal coated recorded as a function of immersion time in $K_2SO_4$ and NaCl

| **Solutions** | **Concentration of $Al_2O_3$ [g/l]** | **Time (h)** | | | | |
|---|---|---|---|---|---|---|
| | | ***0.5*** | ***2*** | ***4*** | ***6*** | ***24*** |
| **$K_2SO_4$** | **0** | 2.023 | 2.549 | 4.108 | 6.276 | 8.07 |
| | **20** | 0.102 | 0.106 | 0.117 | 0.502 | 1.467 |
| | **30** | 1.312 | 3.42 | 7.003 | 7.47 | 8.514 |
| **NaCl** | **0** | 2.66 | 3.169 | 4.94 | 6.525 | 7.914 |
| | **20** | 0.414 | 0.775 | 0.882 | 1.461 | 2.241 |
| | **30** | 5.486 | 16.42 | 19.28 | 22.47 | 27.76 |

The results presented in Tables 4 and 5 show the following: a decrease in the values of the resistances ($R_{rev}$) and higher values of the capacitance ($C_{rev}$) as a function of the immersion time. Indeed, by considering the relationship Stern-Geary, the $R_{rev}$ and the corrosion current are inversely related.

The interpretation of the variation of the resistance of the coating ($R_{rev}$) as a function of time can be explained by the progressive formation of the hydration products of the above coating layer leading to a slower decrease of ($R_{rev}$).

On the other hand, the increase in coating resistance values ($R_{rev}$) and a decrease in coating capacity values ($C_{rev}$) in the presence of $Al_2O_3$ particles, are explained by the layer of corrosion products formed on the surface of the composite deposit being thicker and less permeable than in the case of its absence. This results in the reduction of the active surface in direct contact with the corrosive medium, following the incorporation of the particles, or in the increase in the thickness of the layer of corrosion products.

The impedance results are consistent with the results extracted from the polarization curves, the best values being observed in the case of the Ni-$Al_2O_3$ composite coatings, at a concentration of 20 $g.L^{-1}$ whose corrosion rate is minimal.

## 4. CONCLUSION

The Ni-$Al_2O_3$ electroplating method has been successfully carried out, and the results obtained lead us to the following conclusions:

*Electrodeposited aluminium oxide ($Al_2O_3$) is stable, dense, and adherent, a good protector which, when associated with nickel plating baths, tends to reduce the corrosion of the resulting deposits.

*The incorporation of $Al_2O_3$ particles into the metal structure of nickel leads to a composite material, Ni-$Al_2O_3$, which gives the steel substrate significant corrosion resistance.

* The decrease in the corrosion rate is due to the incorporation of Al2O3 particles in the pores of the coating (clogging of the porosity of the coating).

The optimal $Al_2O_3$ concentration for good corrosion properties of steel has been recorded at 20 g.L$^{-1}$.

It should be noted that a concentration of $Al_2O_3$ exceeds 20 g.L$^{-1}$ for the electrodeposition baths, induces an increase in corrosion rate. In addition, corrosion has a less uniform appearance can be attributed to the random distribution of $Al_2O_3$ in the repository, the result of the agglomeration of the particles in the bath. The $Al_2O_3$ particles embedded in the nickel matrix disrupt nickel increase during electroplating.

Electrochemical impedance spectroscopy and potentiodynamic polarization methods are powerful techniques to verify the quality of corrosion protection composite deposits Ni-$Al_2O_3$. The composite deposition Ni-$Al_2O_3$ moves the corrosion potential to values less noble (cathodic displacement) when compared to that of the steel in the two solutions (NaCl and $K_2SO_4$). However, the offset of this potential is remarkably more negative for the submerged slides in NaCl than for those immersed in $K_2SO_4$. The corrosion current density is larger in the middle than 0.5 M sodium chloride medium 0.5M potassium sulfate. This shows the aggressiveness of chlorides whatever the nature of the coatings (composite coating in our case considered a new type of coating).

## REFERENCES

[1] A. C. Ciubotariu, L. Benea, M. Lakatos Varsanyi, and V. Dragan , Electrochim. Acta 53 (2008) 4557.

[2] Arshali Sasi, Manoj Monda, Saurabh Daya, and Sasi Kumar, Mater. Tod. Process. 2 (2015) 3042.

[3] Research funded by the Division of Research and Scientific Cooperation of the DGTRE (2008).

[4] S.A. Ataie, and A. Zakeri, Alloys Compd. 674 (2016) 315.

[5] M. D. Ger, Mater. Chem. Phys. 87 (2004) 67.

[6] T. He, Y. He, H. Li, Z. Su, Y. Fan, and Z. He, Ceram. Int. 44 (2018) 9188.

[7] F. Xia, W. Jia, M. Jiang, W. Cui, and J. Wang, Ceram. Int. 43 (2017) 14623.

[8] R. N. Gupta, A. K. Das, Nagahanumaiah, and S. Henal, Mater. Manuf. Process. 31 (2016) 42.

[9] S. Mahdavi, and S. R. Allahkaram, Alloy. Comp. 635 (2015) 150.

[10] G. Cârâc, L. Benea, C. Iticescu, T. Lampke, S. Steinhäuser, and B. Wielage, Surf. Eng. 20 (2004) 353.

[11] H. Wang, P. Shi, H. Yu, and B. Xu, Phys. Procedia 50 (2013) 225.

[12] I. Tudela, Y. Zhang, M. Pal, I. Kerr, and A. J. Cobley, Surf. Coat. Technol. 259 (2014) 363.

[13] S. Yari, and C. Dehghanian, Ceram. Int. 39 (2013) 7759.
[14] T. J. Tuaweri, and G. D. Wilcox, Trans. Imf. 85 (2007) 245.
[15] Z. Zhang, X. Wu, C. Jiang, and N. Ma, Surf. Eng. 30 (2014) 21.
[16] X. Peng, X. Xu, and J. Wang, Ceram. Int. 44 (2018) 8599.
[17] W. Cui, K. Wang, K. Wang, and P. Wang, Ceram. Int. 44 (2018) 7214.
[18] E. Rudnik, L. Burzyńska, and M. Gębka, Trans. IMF. 89 (2011) 33.
[19] R. Q. Fratari, and A. Robin, Surf. Coat. Technol. 200 (2006) 4082.
[20] S. T. Aruna, V. K. William Grips, and K. S. Rajam, Alloy. Comp. 468 (2009) 546.
[21] A. Lozano Morales, and E. J. Podlaha, Electrochem. Soc. 151 (2004) C478.
[22] K. Helle, F.C. Walsh, Proceedings of the 26th International Congress of Metal Finishing, Birmingham, England (1996).
[23] C. Kerr, D. Barker, F.C. Walsh, and J. Archer, Trans. Inst. Met. Finish. 78 (2000) 171.
[24] A. Hovestad, R. Ansink, and L. J. J. Janssen, Appl. Electrochem. 27 (1997) 756.
[25] A. Hovestad, and L. J. J. Janssen, Appl. Electrochem. 25 (1995) 519.
[26] A. Hovestad, R. J. Heesen, and L. J. J. Janssen, Appl. Electrochem. 29 (1999) 331.
[27] P. Bercot, E. Pena Munoz, and J. Pagetti, Surf. Coat. Technol. 157 (2002) 282.
[28] F. Erler, C. Jacob, H. Romanus, L. Spiess, B. Wielage, T. Lampke, and S. Steinhauser, Electrochim. Acta 48 (2003) 3063.
[29] I. Corni, R. J. Chater, and A. R. Boccaccini, Mater. Sci. 47 (2012) 5361.
[30] L. Chen, L. Wang, Z. Zeng, and J. Zhang, Surf. Coat. Technol. 201 (2006) 599.
[31] B. M. Praveen, and T.V. Venkatesha, Appl. Surf. Sci. 254 (2008) 2418.
[32] A. Sohrabi, A. Dolati, M. Ghorbani, A. Monfared, and P. Stroeve, Mater. Chem. Phys. 121 (2010) 497.
[33] C. Gheorghies, G. Carac, and I. V. Stasi, Optoelectr. Advan. Mater. 8 (2006) 1234.
[34] W. Y. Li, C. Zhang, H. Liao, J. Li, and C. Coddet, Surf. Coat. Technol. 202 (2008) 4855.

***Copyright © 2023 by CEE (Center of Excellence in Electrochemistry)***

***Reproduction is permitted for noncommercial purposes.***